

Dielectric and microstructural properties of BaTiO₃ and Ba_{0.9925}Er_{0.0075}TiO₃ ceramics

Fatin Adila Ismail^{1,2*}, Rozana Aina Maulat Osman^{1,2}, Mohd Sobri Idris^{1,3}, Sanna Taking² and Zul Azhar Zahid Jamal²

¹CoE Frontier Materials Research, School of Material Engineering, Universiti Malaysia Perlis, 01000 Kangar, Perlis, Malaysia

²School of Microelectronic Engineering, Universiti Malaysia Perlis, 02600 Arau, Perlis, Malaysia

³School of Material Engineering, Universiti Malaysia Perlis, 02600 Arau, Perlis, Malaysia

Abstract. BaTiO₃ and Ba_{0.9925}Er_{0.0075}TiO₃ ceramics were investigated regarding their dielectric and microstructure properties via conventional solid state reaction method. The phase pure samples were obtained when heated at 1400°C for overnight. The effect of Er³⁺ doped into BaTiO₃ on dielectric properties and microstructural properties was investigated for composition of BaTiO₃ and Ba_{0.9925}Er_{0.0075}TiO₃. The analysis was made by X-ray Diffraction (XRD), Scanning Electron Microscopy (SEM) and Impedance Analyzer. The XRD patterns of BaTiO₃ and Ba_{0.9925}Er_{0.0075}TiO₃ are phase pure and identical with tetragonal perovskite structure with space group of P4mm. The lattice parameters and unit cell volume of BaTiO₃ increased by doping with Erbium as the crystallite size decreased. Measurements of dielectric properties were carried out as a function of temperature up to 200°C at different frequencies. Ba_{0.9925}Er_{0.0075}TiO₃ exhibit the high value of dielectric constant ($\epsilon=6179$) at Curie temperature (T_c) of 120°C. SEM analysis of BaTiO₃ and Ba_{0.9925}Er_{0.0075}TiO₃ ceramics showed that the grain sizes of BaTiO₃ and Ba_{0.9925}Er_{0.0075}TiO₃ were ranged from 3.3µm-7.8µm and 2.2µm-4.7µm respectively.

1 Introduction

The Barium titanate (BaTiO₃) – based ferroelectric ceramics have gained importance in electronic industry as they have high dielectric constant and offer wide range of applications such as capacitors, sensors, actuators, power transmission devices, memory devices and high energy storage devices [1-2]. BaTiO₃ has a perovskite structure and due to this perovskite structure, BaTiO₃ has intrinsic capability to host different dopant ions with different sizes. The influence of dopant ion depends on the substitutional site (Ba²⁺ or Ti⁴⁺) as well as on the defects itself. The ionic radius of the dopant ion is essential for the determination of the substitutional site of host material. The ions with small ionic radii such as La³⁺ and Ce³⁺ will substitute into A- site whereas the ions with bigger ionic radii such as Lu³⁺ and Yb³⁺ possibly substitute at B site of BaTiO₃ structure. The ions that have amphoteric behaviour such as Y³⁺, Dy³⁺, Ho³⁺ and Er³⁺ can occupy both cation lattice site in the BaTiO₃ structure [3-4]. The influence of the dopant incorporation into BaTiO₃ as well as the influence of some transition metal and large rare earth ions in the structural and electrical properties of BaTiO₃ ceramics has been extensively investigated. Among them, Erbium (Er³⁺) has been widely used due to its great technological interest. It has been previously reported by Leyet et. al. [5] that with the Erbium cation incorporation into

BaTiO₃ crystalline lattice according to the formula Ba_{1-x}Er_xTiO₃, increase in dielectric constant is observed. This suggests that the incorporation of Er³⁺ into BaTiO₃ crystalline lattice can be greatly improve the dielectric properties of BaTiO₃. The aim of this work is to investigate the structural and electrical properties of Er doped BaTiO₃ as a function of the Er³⁺ concentration as well as to correlate the structure properties of pure BaTiO₃ and Ba_{0.9925}Er_{0.0075}TiO₃.

2 Experimental

BaTiO₃ and Ba_{0.9925}Er_{0.0075}TiO₃ compositions were prepared via conventional solid state reaction method. The chemicals used were high purity of BaCO₃ (99.99% Pure, Sigma-Aldrich), USA), TiO₂ (99.99%, Sigma-Aldrich) and Er₂O₃ (99%, Sigma-Aldrich) powders. BaCO₃, TiO₂ and Er₂O₃ were weighed using A&D Weighing HR250AZ pharma balance. Powder samples were mixed and ground using pestle and mortar. Samples were ground for half an hour by hand using acetone as the medium for mixing. Samples were then pressed into pellets shape by using uniaxial press with 1 tonne pressured. Pellets were then heated in air at high temperature between 1000°C and 1400°C at 5°C/min for overnight. The crystal structures of the samples were confirmed by using X-ray Diffraction (Bruker, D2-Phaser) with Cu K α radiation ($\lambda = 1.5406$). Samples

* Corresponding author: fatinadilaismail@gmail.com

were measured in range of $2\theta = 20^\circ - 80^\circ$ using step size of 0.02. The sintering temperature for electrical measurement was 1300°C for 3 hours with heating and cooling rate of about $5^\circ\text{C}/\text{min}$ in air. For electrical measurements, the surfaces of sintered pellets were painted with silver conductive paint. The electrical characterization is measured using Impedance Analyser (Hioki IM3570) from room temperature to 200°C at 1kHz, 10 kHz and 100 kHz. The microstructure was studied by using Scanning Electron Microscopy (SEM). The SEM micrographs were obtained using a JEOL JSM-6460LA SEM. The grains size distribution was measured using SEM image analysis software, Smile View.

3 Results and Discussions

3.1 XRD Analysis

Fig. 1 shows the X-ray Diffraction (XRD) patterns of BaTiO_3 and $\text{Ba}_{0.9925}\text{Er}_{0.0075}\text{TiO}_3$ samples heated at 1400°C for overnight. The XRD patterns show similar XRD pattern with an early reported BaTiO_3 tetragonal perovskite structure [6, 7]. The XRD patterns are the

same and show the single phase tetragonal perovskite structure with space group of $P4mm$. The lattice parameters and unit cell volume for the sample BaTiO_3 composition sintered at 1400°C were $a = 3.9918 \text{ \AA}$ and $c = 4.0338 \text{ \AA}$ and unit cell volume, $V = 64.28 \text{ \AA}^3$. The lattice parameters and unit cell volume for the sample $\text{Ba}_{0.9925}\text{Er}_{0.0075}\text{TiO}_3$ composition sintered at 1400°C were $a = 3.9940 \text{ \AA}$ and $c = 4.0362 \text{ \AA}$ and unit cell volume, $V = 64.38 \text{ \AA}^3$. Table 1 shows the structure parameters of BaTiO_3 and $\text{Ba}_{0.9925}\text{Er}_{0.0075}\text{TiO}_3$ obtained. An increase in lattice parameters of BaTiO_3 as doped with Er can be observed. The average crystallite size values of pure BaTiO_3 and Erbium doped BaTiO_3 ceramics, revealing there is a decrease in the size suggesting the effect of dopant on crystallite size of BaTiO_3 . The crystallite sizes were evaluated through the Scherrer's equation. It is commonly determined by measuring the Bragg's peak width at the half maximum intensity and by using the Scherrer's formula (Eq. 1), where d is the crystalline size, λ is the wavelength of the x-ray, β is the peak width at the half maximum intensity and theta is the Bragg's angle [7].

$$d = \frac{0.9\lambda}{\beta \cos\theta} \quad (1)$$

Table 1. Structural parameters of BaTiO_3 and $\text{Ba}_{0.9925}\text{Er}_{0.0075}\text{TiO}_3$ prepared samples and their calculated crystallite sizes.

Sample	$a \text{ (\AA)}$	$c \text{ (\AA)}$	$V \text{ (cm}^3\text{)}$	Crystallite size (\AA)
BaTiO_3	3.9918(3)	4.0338(5)	64.28(2)	1068.44
$\text{Ba}_{0.9925}\text{Er}_{0.0075}\text{TiO}_3$	3.9940(3)	4.0362(5)	64.38(1)	931

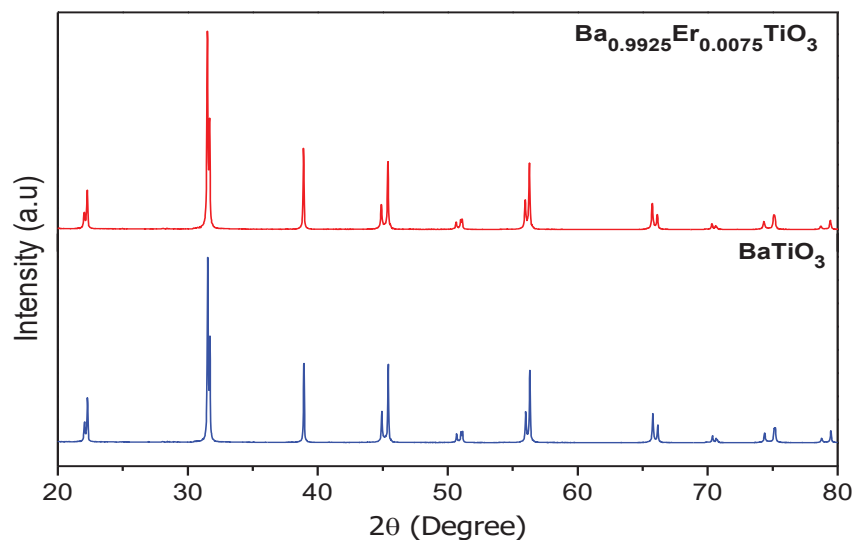


Fig. 1. XRD pattern of BaTiO_3 and $\text{Ba}_{0.9925}\text{Er}_{0.0075}\text{TiO}_3$ heated at 1400°C

3.2 Electrical Analysis

The dielectric behavior and dielectric loss as a function of temperature for the sintered pellets of BaTiO_3 and $\text{Ba}_{0.9925}\text{Er}_{0.0075}\text{TiO}_3$ at 1 kHz is shown in Fig. 2. It can be observed that by doping, the permittivity increase from

5194 to 6502 for BaTiO_3 and $\text{Ba}_{0.9925}\text{Er}_{0.0075}\text{TiO}_3$. The Curie temperature, T_C increased by doping which is from 110°C to 120°C for BaTiO_3 and $\text{Ba}_{0.9925}\text{Er}_{0.0075}\text{TiO}_3$ respectively. Increase in T_C may be due to the misfit between the grain core and the grain shell give rise to stresses and shift the Curie point to higher temperature

as suggested by Hwang et. al [8]. Some of rare earth doping that increase the T_C are Yb doped BaTiO₃ and Lu doped BaTiO₃ which is quite similar to the current Er doped BaTiO₃ system. Based on Fig. 2, an increase in dielectric constant from 5194 to 6502 for BaTiO₃ and

Ba_{0.9925}Er_{0.0075}TiO₃ can be observed at 1 kHz. The increase in dielectric constant can be due to the modifications in the grain size, resulting from the incorporation of the erbium in the BaTiO₃ structure [5].

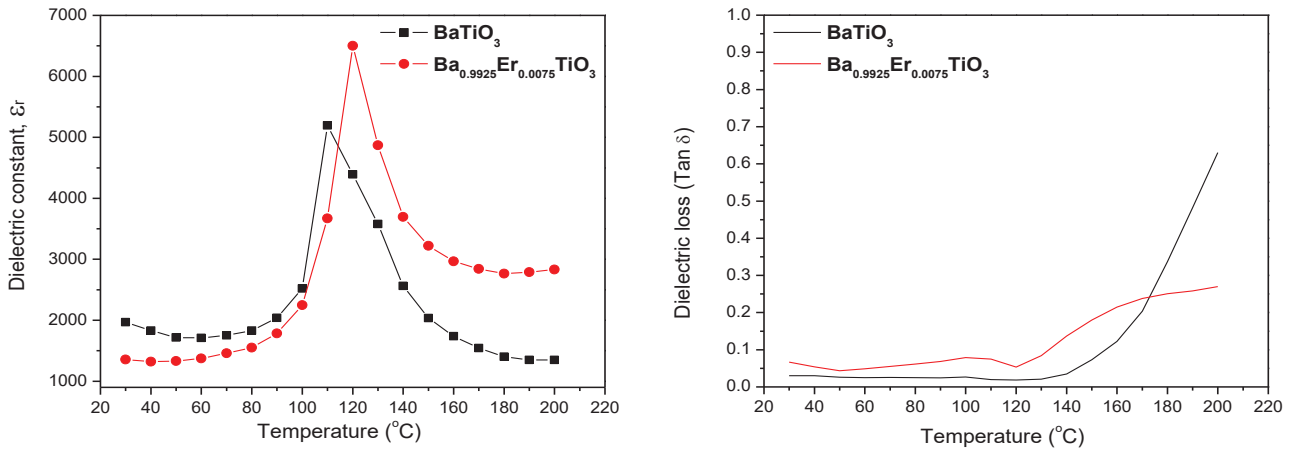


Fig. 2. Dielectric constant and dielectric loss of BaTiO₃ and Ba_{0.9925}Er_{0.0075}TiO₃ at 1 kHz

As for the dielectric loss, it can be seen that the dielectric loss of BaTiO₃ and Ba_{0.9925}Er_{0.0075}TiO₃ were less than 0.1 at temperature below 120°C. Much higher dielectric loss which is more than 0.1 observed at higher temperature

above 120°C up to 200°C. Table 2 summarizes the dielectric constant values and T_C of BaTiO₃ and Ba_{0.9925}Er_{0.0075}TiO₃ at different frequencies. The dielectric constant values are decreased as the frequency increased.

Table 2. Dielectric constant and T_C of BaTiO₃ and Ba_{0.9925}Er_{0.0075}TiO₃ at different frequencies.

Sample	Dielectric constant	Curie temperatre, T_C	Frequency
BaTiO ₃	5194	110°C	1kHz
	5072		10kHz
	4880		100kHz
Ba _{0.9925} Er _{0.0075} TiO ₃	6502	120°C	1kHz
	6179		10kHz
	5891		100kHz

Ba_{0.9925}Er_{0.0075}TiO₃ shows the highest dielectric constant at 1 kHz which increased by almost 1000 as compared to the BaTiO₃. The T_C of Ba_{0.9925}Er_{0.0075}TiO₃ increased by 10°C from T_C of BaTiO₃. However, as the frequency increased, the dielectric constant values decreased. The decreasing dielectric constant values across the frequencies may be due to space charge polarization as reported by Ganguly et al. [9]. Fig. 3(a) shows the variation of capacitance value for undoped BaTiO₃ and Er doped BaTiO₃ at x=0.0075. The capacitance values

increases from about $\sim 3 \times 10^{-9}$ Fcm⁻¹ to $\sim 4 \times 10^{-9}$ Fcm⁻¹ by doping Er into BaTiO₃. These results are consistent with the results of dielectric constant. Fig. 3(b) shows the conductivity values of BaTiO₃ and Ba_{0.9925}Er_{0.0075}TiO₃ at specific temperatures from 30°C to 200°C. The conductivity was between $\sim 10^{-7}$ Scm⁻¹ and $\sim 10^{-6}$ Scm⁻¹. The conductivity of BaTiO₃ shows the trend for insulator behavior which increased from room temperature to T_C and decreased after T_C . For Ba_{0.9925}Er_{0.0075}TiO₃, the conductivity of samples shows

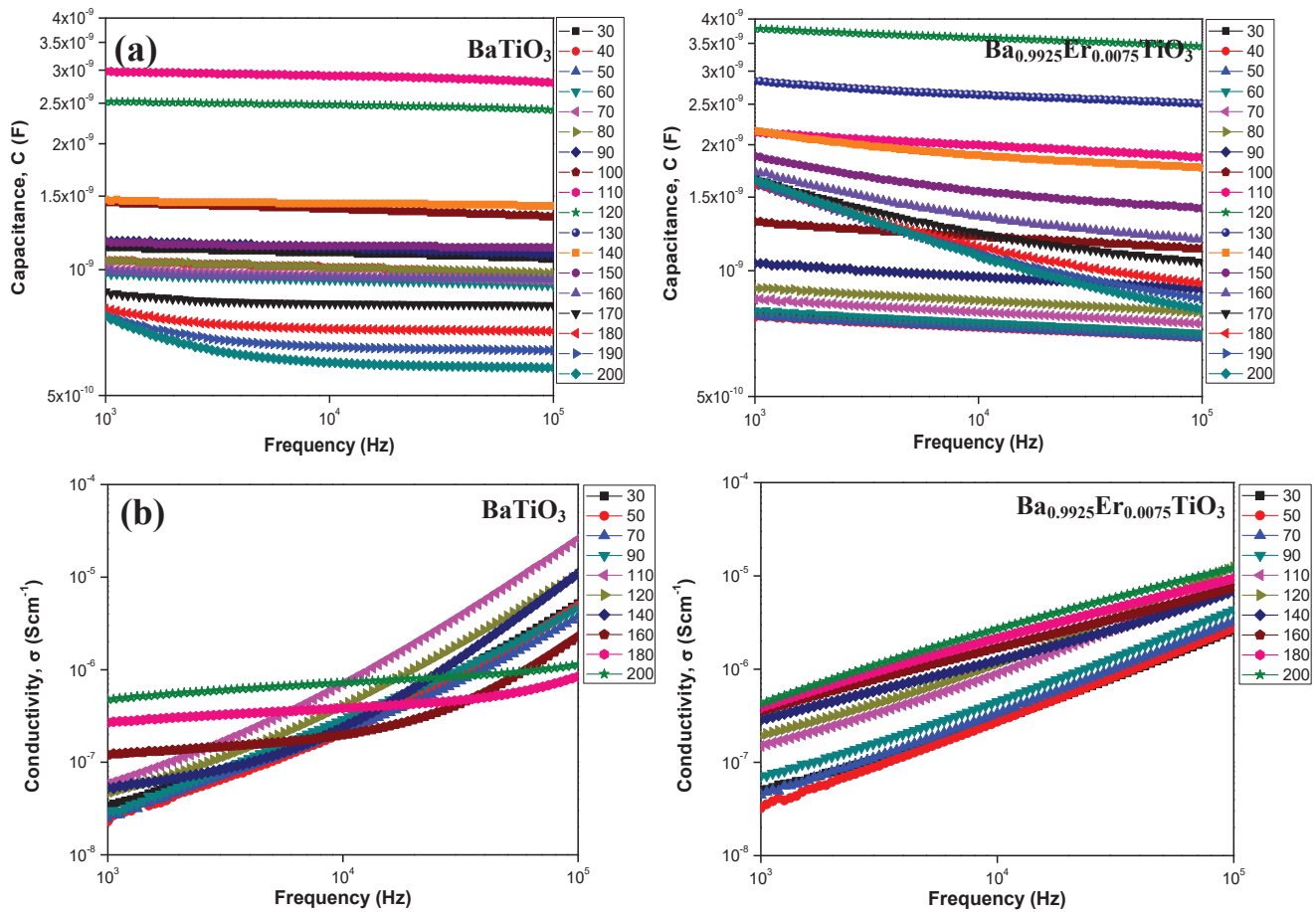


Fig. 3. a) Capacitance and b) conductivity of BaTiO₃ and Ba_{1-0.9925}Er_{0.0075}TiO₃ as a function of frequencies at different temperature

the typical ceramic behavior which increased as the temperature increased.

3.3 Microstructural Analysis

Fig. 4 shows that the surface morphology of sintered BaTiO₃ and Ba_{0.9925}Er_{0.0075}TiO₃ by using SEM. The relation between dielectric constant and the grain size of sintered BaTiO₃ and Ba_{0.9925}Er_{0.0075}TiO₃ were observed. These micrographs were captured by 1000x magnification using Secondary Electron (SE) mode.

From Fig. 4(a) and 4(b), the irregular shape of grains can be seen for both samples. However, there is difference in the grain size as shown in grain size distribution graph in Fig. 5(a) and 5(b). The grain size of BaTiO₃ was in between 3.3μm-7.8μm and the grain size for Ba_{0.9925}Er_{0.0075}TiO₃ was ranged from 2.2μm-4.7μm. The grain size of Ba_{0.9925}Er_{0.0075}TiO₃ is much smaller as compared to BaTiO₃. Therefore, the dielectric constant of Ba_{0.9925}Er_{0.0075}TiO₃ sample is much higher than BaTiO₃ samples.

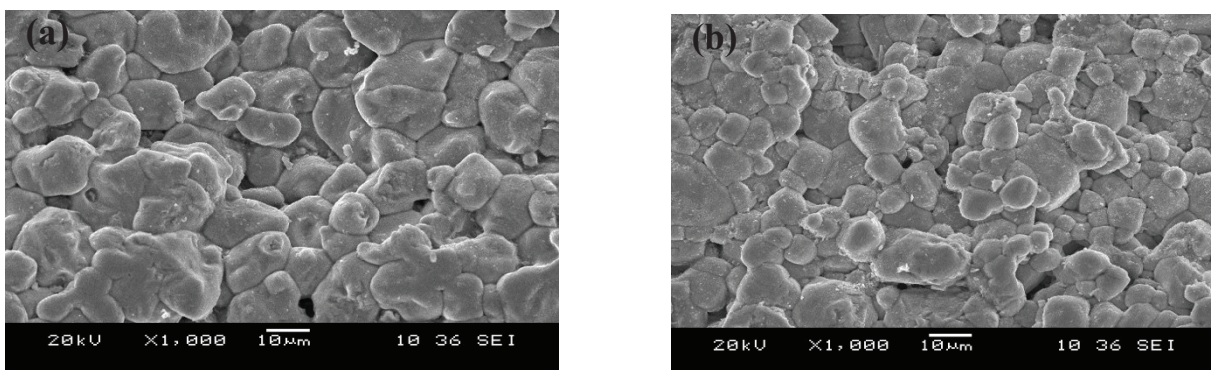


Fig. 4. Scanning electron micrographs of sintered (a) BaTiO₃ and (b) Ba_{1-0.9925}Er_{0.0075}TiO₃ at 1000x magnification

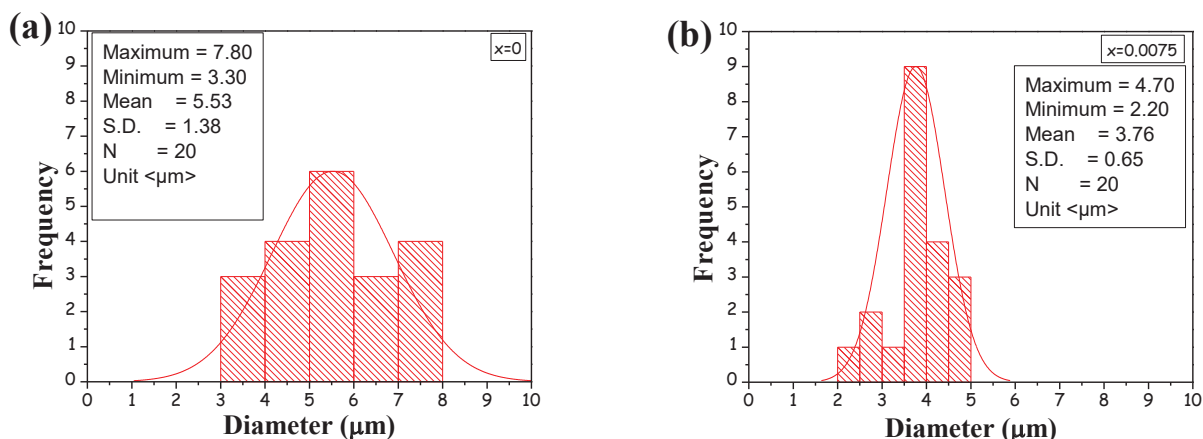


Fig. 5. Grain size distribution of sintered (a) BaTiO₃ and (b) Ba_{1-0.9925}Er_{0.0075}TiO₃ at 1000x magnification

4 Conclusions

Doping study using Erbium doped BaTiO₃ was studied with the effect of small amount of Er to the A-site of BaTiO₃. The dielectric behaviour of BaTiO₃ improved by doping. The highest dielectric constant observed at Er doped BaTiO₃ with dielectric constant maximum at T_C about 120°C which is 6502. As for dielectric loss, the value is lower than 0.1. Besides, the capacitance and conductivity also improved significantly. The capacitance increased from $\sim 3 \times 10^{-9}$ Fcm⁻¹ to $\sim 4 \times 10^{-9}$ Fcm⁻¹. The conductivity was between $\sim 10^{-7}$ Scm⁻¹ and $\sim 10^{-6}$ Scm⁻¹. The effects of Erbium doping on the microstructural properties were verified as the grain size decreased as Er doped into BaTiO₃. The grain size of BaTiO₃ was in between 3.3 μm - 7.8 μm which is larger as compared to the grain size for Ba_{0.9925}Er_{0.0075}TiO₃ ranged from 2.2 μm - 4.7 μm. Finally, it can be concluded that by doping Er into BaTiO₃, the dielectric properties were improved and can be correlated with microstructure properties.

The authors are grateful to Universiti Malaysia Perlis (UniMAP), for giving opportunities to do this research project, Ministry of High Education (MOHE) for funding on Exploratory Research Grant Scheme, FRGS (Grant No: 9010-00032).

References

1. G. H. Haertling, Journal of the American Ceramic Society, **82(4)**, 797-818 (1999).
2. A. J. Moulson and J. M. Herbert, *Electroceramics: Materials, Properties, Applications* (1990).
3. M. T. Buscaglia, M. Viviani, V. Buscaglia, C. Bottino and P. Nanni, Journal of the American Ceramic Society, **85(6)**, 1569-1575(2002).
4. P. Yongping, Y. Wenhui, and C. Shoutian, Journal of Rare Earths, **25**, 154-157(2007).
5. Y. Leyet, R. Peña, Y. Zulueta, F. Guerrero, J. Anglada-Rivera, Y. Romaguera, and J. P. Cruz, Materials Science and Engineering: B, **177(11)**, 832-837(2012).
6. N. A. Hamid, R. A. M. Osman, M. S. Idris and T.Q. Tan, Materials Science Forum, **819** (2015).
7. Y. Leyet, L. Aguilera, A. Perez-Rivero, F. Guerrero and M. I. B. Bernardi, Rev. Cub. Quim, **22**,62-72 (2010).
8. J. H. Hwang, S. K. Choi and Y. H. Han, Japanese Journal of Applied Physics, **40(8)**, 4952 (2001).
9. M. Ganguly, S. K. Rout, P. K. Barhai, C. W. Ahn and I. W. Kim, Phase Transitions, **87(2)**, 157-174 (2014).